



Original Article

Design and Fabrication of an X-Band Low Noise Amplifier Using FR-4 for Military Radar and Ground Station Receiver Applications

Ta Phuong Linh^{1,*}, Tran Chinh Doan², Bach Gia Duong²

¹*Vietnam National Space Center, Vietnam Academy of Science and Technology,
Building A6, 18 Hoang Quoc Viet, Hanoi, Vietnam*

²*VNU University of Engineering and Technology, 144 Xuan Thuy, Cau Giay, Hanoi, Vietnam*

Received 18 August 2021

Revised 19 September 2021; Accepted 19 September 2021

Abstract: The low noise amplifier (LNA) plays an important role in the radiofrequency receiver front-ends, its main function is to amplify the weak receiving signal from the ground noise, as well as improving the receiver sensitivity. For LNAs which operate in the frequencies higher than the S-band, the printed circuit board (PCB) with high cost substrate materials have been used in almost designs so far, thus increasing the total price of the entire receiving unit. This paper introduces a new approach, in which a LNA has been designed using the FR-4 material, a common, low-cost substrate in PCB fabrication. The proposed LNA will maintain the quality of all of the important parameters such as gain, noise figure in compared with the LNAs designed by high cost material substrates. The stepped impedance matching technique is used in order to reach a balance between the circuit dimension and its efficiency. The frequency range of the proposed LNA lies within the X-band, which is a suitable range for military RADAR applications. Furthermore, it is possible to apply the desired LNA in the ground station receiver front-ends of a Low Earth Orbit (LEO) Earth Observation Satellite system.

Keywords: Low noise amplifier, LNA, FR-4, RADAR, X-band, receiver front-ends.

1. Introduction

The low noise amplifier (LNA) is the foremost component of the receiver front-end circuitry of many communication systems. It acts as a first gain stage, in which the main function is boosting the

* Corresponding author.

E-mail address: talinhpuong@gmail.com

<https://doi.org/10.25073/2588-1124/vnumap.4670>

receiving signal from the noise floor to a sufficient level for succeeding processing. In LNA design, the two most important parameters are gain and noise figure (NF), in which the former determines the LNA's performance and the latter directly affects to the sensitivity of the receiver. Furthermore, other parameters need to be compromised, such as linearity, power consumption, dynamic range and impedance matching. Most of the today microwave LNAs are manufactured using printed circuit board (PCB) technology, in which the microstrip is the most widely applied transmission line due to its advantages such as easy to fabricate, easy to do the impedance matching, and allows integrated circuit design. In designing low-frequency microstrip PCB circuits, the Flame Retardant #4 (FR-4) epoxy glass is very popular to use as the board's dielectric substrate because of its considerable merits, namely reasonable cost, linear loss tangent over a wide frequency span, and relatively good mechanical properties [1]. However, in high frequency ranges (for example, X-band and above), the FR-4 loss tangent becomes non-linear and the material provides a much higher attenuation in comparison to that in lower frequency ranges, for example, the attenuation is 0.04 at 2 GHz and 0.2 at 10 GHz [2]. Therefore, it is challenging to apply the FR-4 material in high frequency circuits.

There are various researches related to designing LNA at X-band, for instance: Girlando et al (2004) introduced an X-band LNA which has the operation frequency of 8 GHz to 12 GHz, with the corresponding noise figures of 2.6 and 4.7 dB, and the corresponding power gain of 11.5 and 8 dB [3]. Complicated, multi-staged LNA topologies with the achieved gain of more than 25 dB and NF of below 2 dB are presented by Thrivikraman et al [4] and Giannini et al [5], respectively. Adabi and Niknejad [6] designed an LNA topology that has the gain of 20.5 dB at 8.8 GHz and the NF of approximately 1.5 dB. All of the mentioned works are well-designed, but with a fairly high level of complexity and none of them using FR-4 for the substrate.

Based on the aforementioned analysis of the advantages and drawbacks of FR4 and a careful study of printed circuit manufacturing in Vietnam, we realized that it is possible to fill the high-frequency gap of FR-4 by using this dielectric material to design and fabricate an X-band microstrip LNA with simplicity and low cost, while maintaining the quality of all of the LNA key parameters, and it is the purpose of this research. The FR-4 X-band LNA can be applied for both military radars and satellite receiver's front-ends with following expected parameters:

- Operation frequency range: 10 GHz ÷ 12 GHz
- Gain: Better than 10 dB in the entire operation frequency range
- Return loss: Lower than -10 dB in the entire operation frequency range

2. Circuit Design

2.1. Design of the LNA Topology

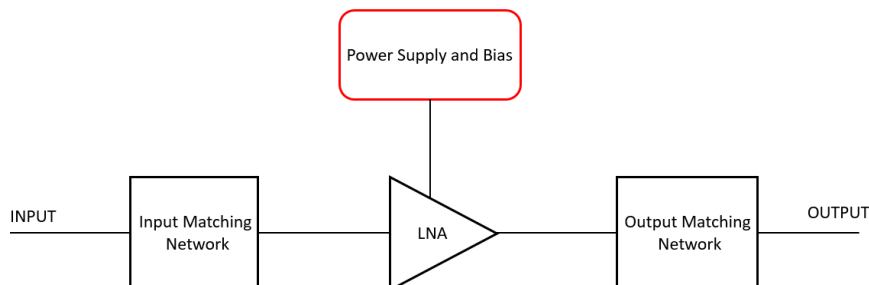


Figure 1. Block diagram of the LNA (redrawn from [7]).

The block diagram of the LNA and the related components are illustrated as follows.

As can be seen in Figure 1, the LNA are matched at the input and output terminals by matching networks. The power supply and bias unit are required to setting and biasing the transistors in the LNA to their operation region.

The transistor served as the active device of the LNA unit can be classified into bipolar junction transistor (BJT) and field effect transistor (FET), where the former is a current controlled device and the latter is a voltage controlled device [8]. The FET, in turn, is divided to several types: metal-semiconductor (MESFET), metal-oxide semiconductor (MOSFET) and high-electron mobility transistor (HEMT) known as a heterostructure FET. Used in most of the LNA applications of above 2.4 GHz, the FET is designed and fabricated by several semiconducting materials, such as gallium arsenide (GaAs) and silicon-germanium (SiGe).

Our desired LNA should have relatively high gain and low noise figure. Moreover, as for a LNA, the output power does not need to be high. Based on these criteria, the Hetero Junction Field Effect Transistor (HJFET) of the model NE3515S02 has been chosen. This transistor provides high gain and very low noise figure, as well as the output power of average level. In addition, its 4-pins configuration provides convenience in circuit design, as well as easy mounting on the conductive layer of the PCB with conventional solder tin. To set the device in its active region, the designed parameters for DC biasing are: $V_{DS} = 2V$ and $I_D = 40mA$. Thus, in this case, the gate to source voltage (V_{GS}) is $-0.2V$ and the dissipated power is lower than $150mW$. Based on the fact that our proposed LNA is a small signal amplifier device, these values allow the operation point lies well in the linear region of the transistor in order to operate as a class A amplifier, thus, the output power is far below the 1-dB compression point (P_{1dB}) value and the saturation level, which can be referred in the NE3515S02 datasheet. Furthermore, the chosen transistor has a high IP3 value so that the intermodulation products could not interfere the fundamental signals.

2.2. Design of the Impedance Matching Network

The purpose of impedance matching is to deliver the maximum amount of power from source to load. To do that, the inputs and outputs of the LNA’s transistors have to be matched with the source impedance (Z_S) and load impedance (Z_L), respectively. The impedance matching network is designed in the case Z_S and Z_L equal to $Z_0 = 50 \Omega$, in which, Z_0 is the characteristic impedance of the transmission line. Figure 2 illustrates the matching network of each stage of the LNA:

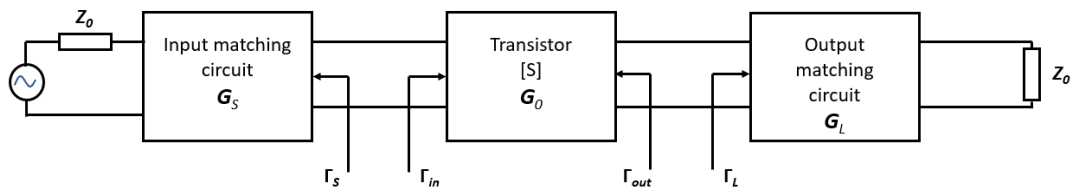


Figure 2. Block diagram of the LNA’s matching network [9].

In the above figure, the transistors of the LNA can be modelled as two-port networks, in which, the inputs and outputs reflection coefficients are in turn Γ_{in} and Γ_{out} (equivalent to S_{11} and S_{22} of the scattering matrix). These values are complex numbers and the normalized values can be read from the transistor’s datasheet. Thus, the inputs and outputs complex impedances of the transistor can be calculated as [9]:

$$Z_{in} = Z_0(1+S_{11})/(1-S_{11}) \tag{1}$$

$$Z_{out} = Z_0(1+S_{22})/(1-S_{22}) \quad (2)$$

In order to match properly, the output impedance or the input matching network and the input impedance of the output matching network should be equal to Z_{in} and Z_{out} , respectively. In this design, we use a combination between the conventional tuning stub impedance matching and stepped impedance matching. The stepped matching technique has significant advantages when applying to microstrip transmission lines at high frequency, such as flexibly frequency tuning by modifying the length of the transmission line and flexibly impedance changing by varying the transmission line's width. Consequently, by using this method, a conventional transmission line with one impedance value through the entire line length can be replaced by several equivalent transmission lines in series, with various impedance values. Thus the total physical length of the matching network's lines can be shortened and the attenuation of the RF signal when travelling through a high loss material like FR-4 will be significantly reduced. A stepped impedance matching network will be shown in the following figure:

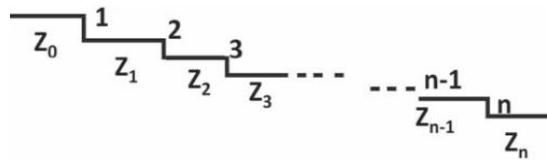


Figure 3. Stepped impedance matching network [10].

In Figure 3, the impedance of the i^{th} transmission line (with the direction toward the termination) can be calculated as follow [11]:

$$Z'_i = Z_i \frac{Z'_{i+1} + jZ_i \tan(\beta l_i)}{Z_i + jZ'_{i+1} \tan(\beta l_i)} \quad (3)$$

where β is the propagation constant, l_i - the physical length of the transmission line and Z_i - the characteristic impedance of the i^{th} transmission line. Table 1 shows the designed values of our impedance matching network:

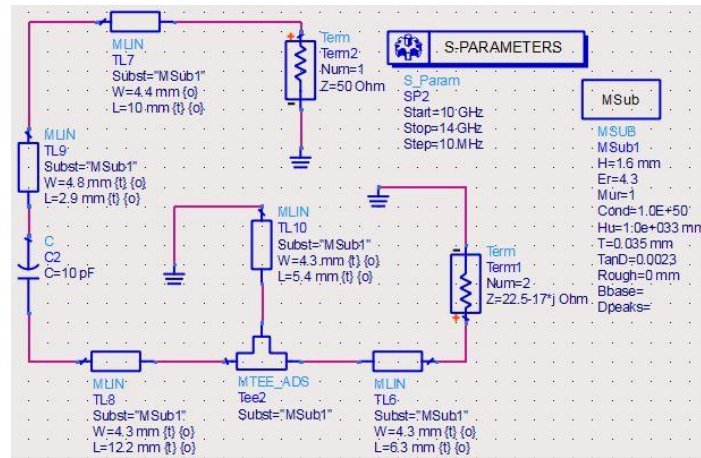
Table 1. The design values of stepped impedance transformer for the input and output matching

Section	Input matching network		Output matching network	
	Width (mm)	Length (mm)	Width (mm)	Length (mm)
1	4.4	10	4.4	14.8
2	4.8	2.9	5.4	2.5
3	4.3	12.2	4.3	12.7
4	4.3	6.3	4.3	16.4

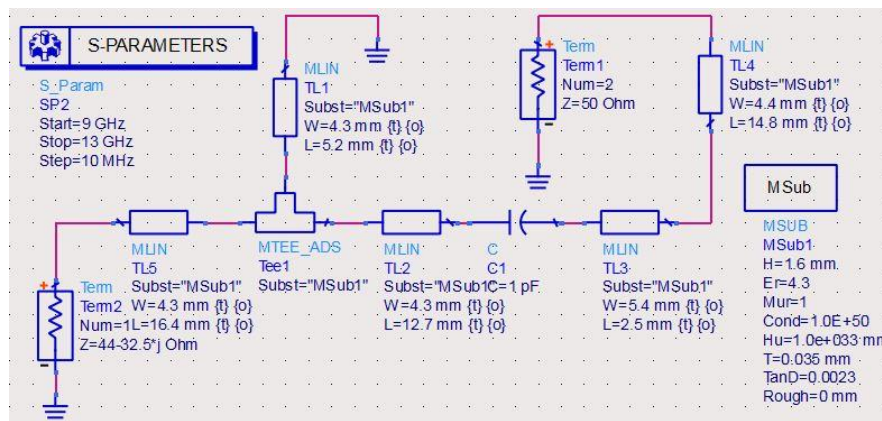
3. Simulation and Experimental Results

3.1. Simulation

The FR-4 dielectric material used in simulation and fabrication has the following attributes: Relative dielectric constant of 4.34, loss tangent of 0.0023, dielectric height of 1.6 mm, conductor thickness of 0.035 mm. The simulation software is Advanced Design System (ADS) 2014, provided by Keysight. The schematic diagrams of the input and output matching networks are shown below:



(a)



(b)

Figure 4. The simulation schematic diagrams of the input matching network (a) and the output matching network (b).

As can be seen in Figure 4, the purpose of the matching networks is to match the 50 Ω impedances of the source and the load to the complex input and output impedances of the NE3515S02 transistor. These values can be calculated from the S-parameter data over frequencies of the transistor, provided by the manufacturer. The simulation results of these matching networks are illustrated as follows:

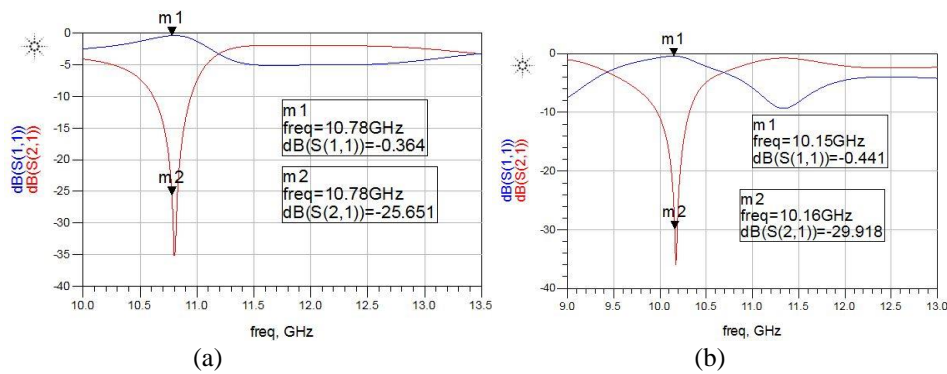


Figure 5. Simulation of gain and return loss of the input matching network (a) and the output matching network (b).

In Figure 5 the input and output matching are done for the range of 10 GHz ÷ 11 GHz, which is the expected operation frequency range of the LNA. This is the reason why we chose the center frequency of the input matching network different from that of the output matching network. The schematic diagram of the simulated LNA is shown below:

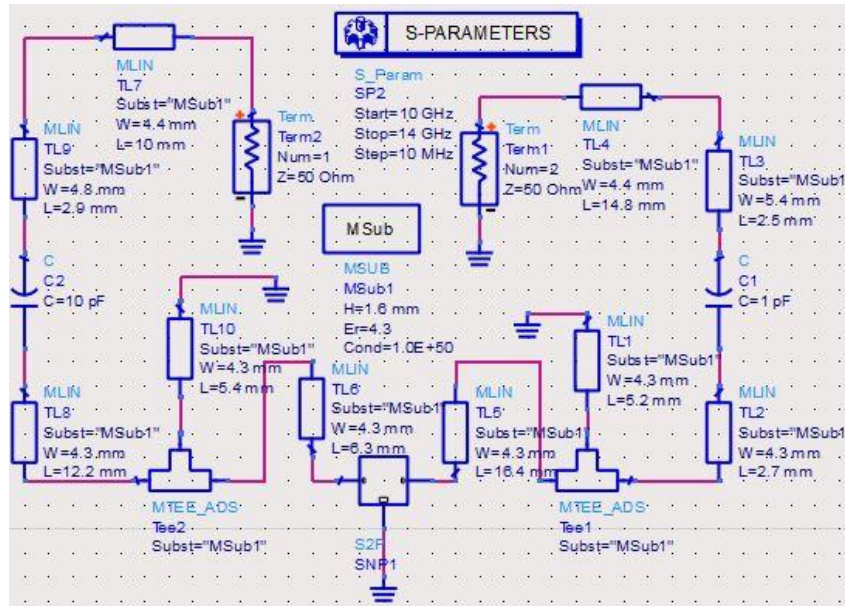


Figure 6. The simulation schematic diagram of the single-stage X-band LNA.

In Figure 6, the stepped impedance transmission lines are combined with short stubs to form the impedance matching networks at the input and output of the transistor. The gain (S_{21}) and return loss (S_{11}) of LNA are shown as follows:

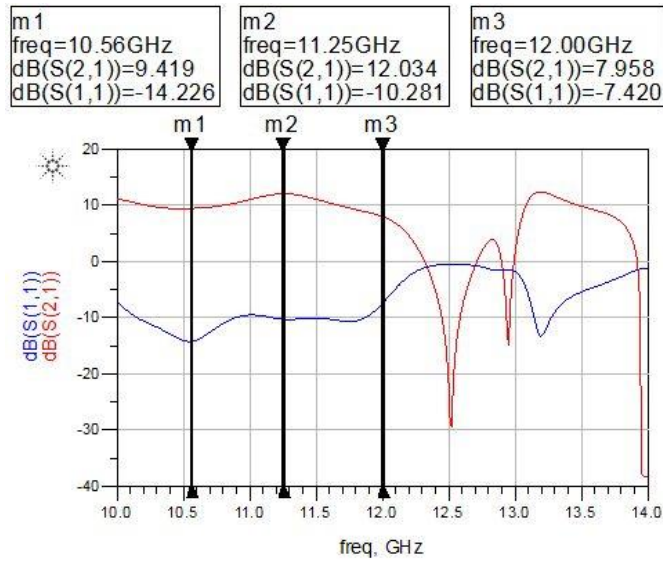


Figure 7. Simulation of gain and return loss of the single-stage LNA over X-band.

Figure 7 demonstrates some operation frequencies of the proposed LNA in the X-band. In detail, the average gain value is around 10 dB from 10 GHz to nearly 12 GHz. The corresponding average return loss is better than -10 dB at the inspected frequency range. Furthermore, in this figure we can see that the passband ripple is about 2.5 dB, which is significantly greater than 1 dB. However, the gain flatness is not the focus of our LNA, so the requirement of this parameter is loosened in the design. Figure 8 presents the noise figure (NF) of the LNA. From this figure, one can see that the simulated NF lies well below or just approximately 1 dB in the investigated frequency band.

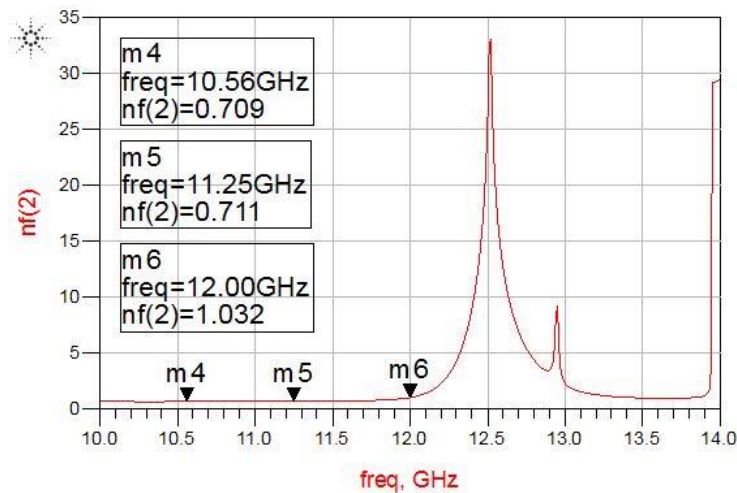


Figure 8. The simulated noise figure of the single-stage LNA.

Figure 9 presents the simulation stability factor (K-factor) of the proposed LNA.

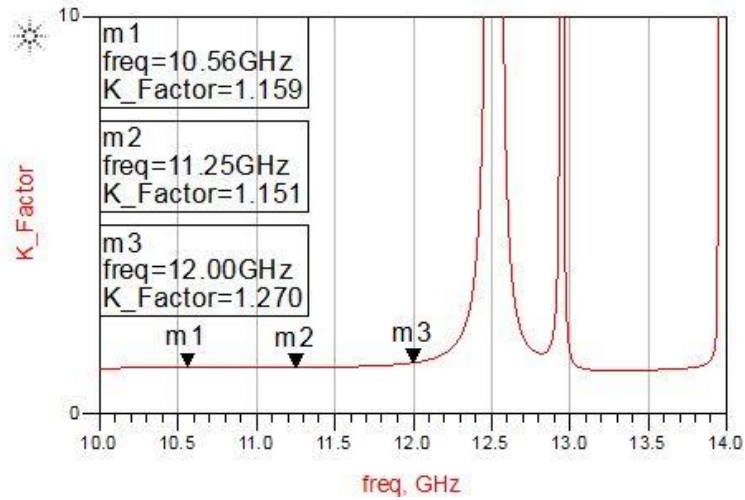


Figure 9. The simulated stability factor of the single-stage LNA.

As shown in Figure 9, the K-factor of the LNA is greater than 1 in the whole operation frequency range. Thus, the LNA is in unconditional stability in this frequency range.

The overall gain of the LNA will be further enhanced by cascading two identical LNA stages. Figure 10 shows the simulated result of the gain and S_{11} in this case:

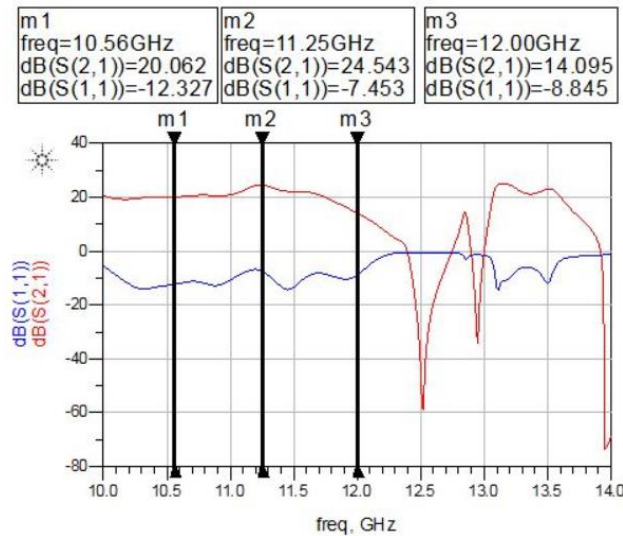


Figure 10. Simulation of gain and return loss of the two-stage LNA over X-band.

A noticeable thing from Figure 10 is that the average gain value over the inspected frequency range is roundly 20 dB. This gain value is enough for applying the two-stage LNA in Radar applications. In addition, the variation over frequencies of the values of S_{11} is stronger than that of the one-stage LNA case, but it is still in an acceptable range.

3.2. Measurement

To verify the design performance after simulation, the LNA is manufactured in our laboratory using the circuit board plotter LPKF ProtoMat C40. The fabricated LNA modules, including a one-stage LNA and an experimental two-stage LNA for further study plan are presented in Figure 11:

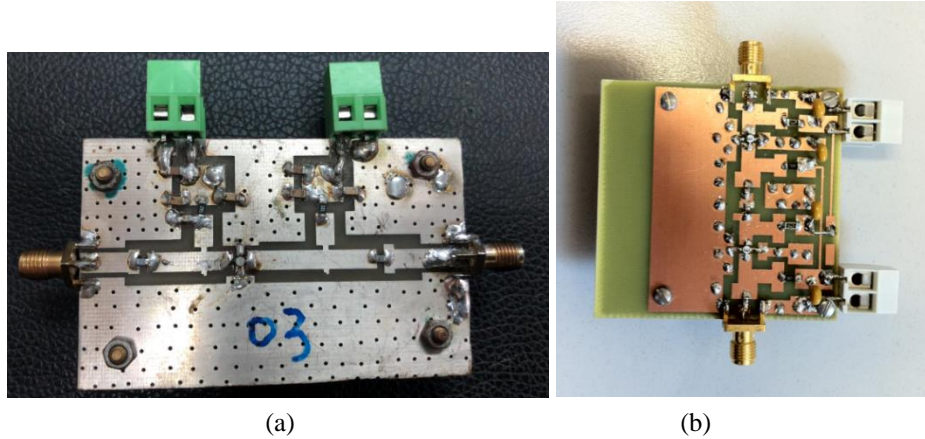


Figure 11. The fabricated LNA modules (a) One-stage (b) Two-stage.

The test and measurement process is carried out by the Keysight E8257D Signal Generator as the signal source and the Keysight N9917A FieldFox Handheld Microwave Analyzer as the signal sink. After going through the LNA, the receiving signal is inputted and displayed on the N9917A’s screen at the frequency domain as illustrated in the below figure:

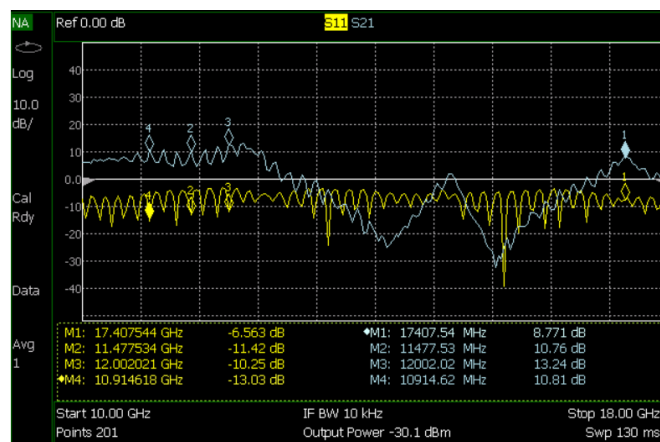


Figure 12. The measured return loss and gain of the one-stage LNA.

From Figure 12 it is clearly seen that the measured results of gain and input reflection coefficient are well agreed with the simulation results shown in Figure 7, in which the measured gains are vibrated around 10 dB from the frequency range of 11 GHz – 12 GHz and the corresponding marker points of the S_{11} stated that the values of better than -10 dB have been obtained. The measured noise figure is around $1.2 \text{ dB} \div 1.5 \text{ dB}$ in the investigated frequency range and it is suitable to the simulated result.

The fluctuations of the S-parameters measured plots are majorly caused by the instability of the grounding of the experimental LNA module; this detrimental effect can be reduced significantly in the final model with a metal case enclosing the LNA and the module’s grounding is soldered to the case’s

chassis. Furthermore, the thermal noise of the N9917A itself will contribute in a minor portion to the overall fluctuation of the plots.

Table 2 compares the LNA parameters of our work with some other studies:

Table 2. Comparison of results

Center Frequency (GHz)	Input reflection coefficient (dB)	Gain (dB)	Noise figure (dB)	Reference
10.9	-13	11	~ 1.5	This work
10	-10	10	< 2	[4]
9	-9	20	~1.5	[6]
10	-18	19.5	~1.3	[12]
7	-11	15	< 2.6	[13]

Based on the suitability between the simulation and experimental results of the one-stage LNA, and the simulation result of the two-stage LNA in Figure 10, the experimental two-stage LNA module has the expected forward gain of over 20 dB and input reflection coefficient of better than -10 dB. Depending on the mission requirements, the dimensions of the LNA module can be further minimized by changing the topologies of the impedance matching networks. Theoretically, this two-stage module can be applied for ground station receiver frontends, as well as X-band military radars. In the radar case, an input protection circuit should be integrated at the input of the LNA module in order to prevent the receiver frontend LNA from desensitization, or even destruction when a high-power level receiving signal suddenly comes to the input. The protection using PIN Diode Limiters is being considered as the most promising method in our case. The detailed analysis and measured results of the two-stage LNA module will be presented in further research.

4. Conclusion

This paper presented the design, simulation and fabrication of an X-band low noise amplifier used for military radar applications, as well as satellite receiver's front-ends. By using the common FR-4 substrate, the compromise between cost and LNA efficiency at high frequency has been achieved while maintaining the quality of the LNA's important parameters. The LNA showed wideband characteristic with the averaged gain of approximately 10 dB and an acceptable return loss of -10 dB. The simulated and measured results of the one-stage LNA topology are presented and compared. The high degree of the agreement between those results suggest that the proposed LNA can be operated in practice.

An experimental two-stage LNA is also being presented, in which the wideband gain of 20 dB and input reflection coefficient of better than -10 dB can be reached when cascading two similar amplifier stages as showed in the simulation result in Section 3. It can be applied in satellite ground station receiver front-end with good feasibility. However, an input protection circuit is required when considering of the LNA implementation in radar systems, and this is our aim of further works.

References

- [1] A. R. Djordjevic, R. M. Biljic, V. D. Likar-Smiljanic, T. K. Sarkar, Wideband Frequency-domain Characterization of FR-4 and Time-domain Causality, IEEE Transactions on Electromagnetic Compatibility, Vol. 43, No. 4, 2001, pp. 662-667, <https://doi.org/10.1109/15.974647>

- [2] E. L. Holzman, Wideband Measurement of The Dielectric Constant of An FR-4 Substrate Using A Parallel-coupled Microstrip Resonator, *IEEE Transactions on Microwave Theory and Techniques*, Vol. 54, No. 7, 2006, pp. 3127-3130, <https://doi.org/10.1109/TMTT.2006.877061>
- [3] G. Girlando, G. Ferla, E. Ragonese, G. Palmisano, Silicon Bipolar LNAs in The X and Ku Bands, 9th International Conference on Electronics, Circuits and Systems, 2002, pp. 113-116.
- [4] T. K. Thirvikraman, W. L. Kuo, J. P. Comeau, A. K. Sutton, J. D. Cressler, P. W. Marshall, M. A. Mitchell, A 2 mW, Sub-2 dB Noise Figure, SiGe Low-Noise Amplifier for X-band High-Altitude or Space-based Radar Applications, 2007 IEEE Radio Frequency Integrated Circuits (RFIC) Symposium, 2007, pp. 629-632.
- [5] F. Giannini, E. Limiti, A. Serino, V. Dainelli, A Medium-power Low-noise Amplifier for X-band Applications, 34th European Microwave Conference, 2004, pp. 37-39.
- [6] E. Adabi, A. M. Niknejad, CMOS Low Noise Amplifier with Capacitive Feedback Matching, 2007 IEEE Custom Integrated Circuits Conference, 2007, pp. 643-646.
- [7] T. V. Hoi, B. G. Duong, Study and Design of Wide Band Low-noise Amplifier Operating at C Band, *VNU Journal of Science: Mathematics - Physics*, Vol. 29, No. 2, 2013, pp. 16-24, http://repository.vnu.edu.vn/handle/VNU_123/56223
- [8] Junction Field Effect Transistor, https://www.electronics-tutorials.ws/transistor/tran_5.html (accessed on: August 16th, 2021).
- [9] D. M. Pozar, Design of Microwave Amplifiers and Oscillators, *Microwave Engineering*, John Willey and Son, New York, 2005, pp. 600-654.
- [10] B. Sindam, P. K. Sharma, J. Raju, Design and Analysis of Stepped Impedance Transformer from Air Filled Waveguide to Dielectric Filled Waveguide for High Power Microwave Window Applications, *Materials Research Express*, Vol. 1, No. 1, 2014, <https://doi.org/10.1088/2053-1591/1/1/015701>
- [11] G. L. Ning, Z. Y. Lei, L. J. Zhang, R. Zou, L. Shao, Design of Concurrent Low-noise Amplifier for Multi-band Applications, *Progress In Electromagnetics Research C*, Vol. 22, 2011, pp. 165-178, <https://doi.org/10.2528/PIERC11052405>
- [12] N. Snir, N. B. Helmer, R. Pasternak, D. Regev, A Packaged X-band Low Noise Amplifier, 2009 IEEE International Conference on Microwaves, Communications, Antennas and Electronics Systems, 2009, pp. 1-4.
- [13] N. Sahin, M. B. Yelten, A 0.18 μm CMOS X-Band Low Noise Amplifier for Space Applications, 2017 New Generation of CAS (NGCAS), 2017, pp. 205-208.